

# GENETIC SWITCHES BETWEEN TWO POPULATION WITH REGARDS TO mRNA AND PROTEINS APPLYING MARKOV CHAIN STOCHASTIC MODEL CHECK

Qin He<sup>1</sup>, RubinWang<sup>2</sup>, XiaochuanPan<sup>3</sup>

<sup>1</sup> East China University of Science and Technology, Meilong 130  
[asamiko@aliyun.com](mailto:asamiko@aliyun.com)

<sup>2</sup> East China University of Science and Technology, Meilong 130  
[rbwang@163.com](mailto:rbwang@163.com)

<sup>3</sup> East China University of Science and Technology, Meilong 130  
[pxc@ecust.edu.cn](mailto:pxc@ecust.edu.cn)

## ABSTRACT

*Arc, one virus-like gene, crucial for learning and memory, was discovered by researchers in neurological disorders fields, Arc mRNA's single directed path and allowing protein binding regional restrictively is a potential investigation on helping shuttle toxic proteins responsible for some diseases related to memory deficiency. To study especially the transform between mRNA and proteins, the switching function of the phenotypes, 'normals' multiplying populations and 'persisters', resilient to stress instead of multiplying is of our interest. Mean time to switching (MTS) is calculated explicitly quantifying the switching process in statistical methods combining Hamiltonian Markov Chain(HMC). The model derived from predator and prey with typeII functional response studies the mechanism of normals with intrinsic rate of increase and the persisters with the instantaneous discovery rate and converting coefficients. During solving the results, since the numeric method is applied for the 2D approximation of Hamiltonion with intrinsic noise induced switching combining geometric minimum action method. In the application of Hamiltonian Markov Chain, the behavior of the conversion (between mRNA and proteins through 6 states from off to on ) is described with probabilistic conditional logic formula and the final concentration is computed with both Continuous and Discret Time Markov Chain(CTMC/DTMC) through Embedding and Switching Diffusion. The MTS, trajectories and Hamiltonian dynamics demonstrate the practical and robust advantages of our model on interpreting the switching process of genes (IGFs, Hax Arcs and etc.) with respects to memory deficiency in aging process which can be useful in further drug efficiency test and disease curing.*

## KEYWORDS

*switching model, mean time to switching, Hamiltonian Markov Chain, geometric minimum action method.*

## 1. INTRODUCTION

In cell biology, non-equilibrium stochastic process is of interest since the observation of experimental results are becoming of higher resolution, studying the molecules both with imaging and expression data are often conducted in both single and population (thousand) order, which basically described in stochastic process whether on a discrete or continuous scale with status changes either genotypically or phenotypically. Many problems are thus studied related

to status switching, including cell regulatory networks[1], signal re-sponse on excitability and inhibition[2], (convinced by translational and transcriptional burst of expression for instances.), metastability among populations, (binding of ligands and proteins, forming of polymerases and etc.).In this paper, we focus on the interaction among genes, mRNA, proteins and etc. To be more specific, while the switching problem among molecules can be studied on geno-type, including sequencing for single RNA, alignments and binding considering condons

and etc, we stay on the switching with expres-sion (concentration) only, which is simplified as modified population problem using Lotka-Volterra equations[3] of two populations only. Thus, rather than the competitor model(for instances, cell bifurcations.), we applied simulation of switching on predator model. The model is based on the following basic assumptions: Prey population (promoters) is fed with enough food all the time while the predator population of the predator(the persisters) depends on the size of prey(promoters).

In our paper, we mainly study the interaction of DNA and its interaction with the associated proteins.(Clinical data of Hax1 and HS1 is downloaded from Ensembl gene database[4]). On one hand, the switching model is calculated under the large deviation theory(LDT)[5] combining the least actions. The Markov chain[6] consider the states of the 2D coordinates (x; y) of mRNA numbers and protein numbers referencing the distribution of x, which follows the order  $O(1)$  while PX follows the time scale on  $O(1/e)$  and guaran-teeing the variant of LDT hold with the transform of the expressions in single population. Only considering the process of diffusion case, we study the binding of hax1 with simple switching between on and off status under its interaction with HS1 seen as in the constant environment, i.e. the closed system at mean field. The dimer which can be cancelled out connect the binding between two single population. On the other hand, one numeric method is applied to solve the problem, making compare with the stochastic process[7] on ap-proximation equation of the mean switching time(MST) with the transform between two status (we studied the switching time with four situations, both multiplicative and asymptotic of single population and the binding and degradation between two population.) Again, this method is also calculated based on the Hamiltonians. We give out the MST with respect to  $N/N_c$  denoting N as the population number of interest and  $N_c$  as the threshold of certain status(either of that population or the other population). Since our study only based on data in the process of transforming in the constant environment, extinction is not considered in this paper. To study both intrinsic and extrinsic noise with the exciting and inhibiting bursts is the potential topic in the future. In the following contents, the first chapter is the proposition of the model, based on least action with LDT and MTS approximation with one stochastic differential equation (SDE) [8]separately; And the second chapter gives numeric experiments based on Hamilton Markov Chain[9] computation of the expression data of hax1 and HS1; In the last chapter, the model is described in the normal logic formula with both probabilistic condition model[10] and the results are analysed with both hamiltonian, realization size, convergence, the rewards computation taking the CTMC as Poisson process[11] and the reachability computation with the transfer kernel of switching diffusion[12] through DTMC. In the appendix, there also includes the complete proof of model with action S based on Hamilton not only based on the explicit equation in this paper. Some descriptive statistics and pre-computation based on the data can be accessed through link in availability. As the process related to motor coordination and func-tion, the Hax's function in regulation, B cell's signal transduction can be further studied with more data considering its excitability and metastability functions with stimulation of drugs for instance in the future as well. And one computation applying DTMC withlinear regression on previous work is made as the further extension of the model.

## 2. PROPOSED MODEL

Molecular interactions are studied on phenotypic data of the mRNA and its associated protein in this paper, especially the trajectory of the production of hax1 and HS1 with interaction with each other through least action method combining diffusion process[10]. Furthermore, in solving the equation, one stochastic differentiation equation approximates the analytic solution and calculation of MST[11] based on converging with Hamiltonian quantities, finding three convergence points through eigenvalue of position quantities as well as satisfying  $H = 0$  and  $H_q = 0$  where  $q(P, X; P, Y)$  are momentum quantities. In the 3rd subsection, the transition is illustrated with belief graph first and then convert ratio are utilized in computing the discrete embedding of the continuous temporal logic. As comparison, the third subsection compute the discretized time markov chain as the approximation considering it as a hybrid systems.

## 2.1. Switching model with least action

First of all, we consider the dynamics of population of the interaction involved systems as diffusion[12], and thus the Hamiltonian  $H(x, \theta)$  is computed with the minimization of action (quasi-potential)[13] instead of some other methods, for instance WKB[14]. With the Lagrangian denoted with respect to Hamiltonian according to LDT:

$$L(x, y) = \sup_{\theta \in R_n} (< y, \theta > - H(x, \theta)) = < y, \theta(x, y) > - H(x, \theta(x, y))$$

Due to the maximizer  $\theta(x, y)$  being implicitly defined by  $H_\theta(x, \theta(x, y)) = y$ , we calculate the action from quasi-potential:

$$V(x_1, x_2) = \inf_{\tau > 0} \inf_{\psi \in C_{x_1(0, \tau)}^{x_2} ST(\psi)} = \inf_{\tau > 0} \inf_{\varphi \in C_{x_1(0, 1)}^{x_2} ST(\psi)} = \inf_{\varphi \in C_{x_1(0, 1)}^{x_2} S(\varphi)}$$

So that for any  $\varphi \in C(0, 1)$  the action  $S(\varphi)$  is given by the equivalent four formula:

$$\begin{aligned} S(\varphi) &= \inf_{\tau > 0} \inf_{\psi \in C_{x_1(0, \tau)}^{x_2} ST(\psi)} \\ S(\varphi) &= \sup_{\theta: [0, 1] \rightarrow H(\varphi, \theta)=0} \int_0^1 < \varphi', \theta(\varphi, \varphi') > d\alpha \\ S(\varphi) &= \int_0^1 < \varphi', \theta(\varphi, \varphi') > d\alpha \\ S(\varphi) &= d\alpha, \lambda = \lambda(\varphi, \varphi') \end{aligned}$$

Note that  $L(x, y)$  is the Lagrangian associated with the Hamiltonian  $H(x, \theta)$  with function  $\theta(x, y)$  and  $\lambda(x, y)$  are implicitly defined for all  $x \in D$  and  $y \in R_n \setminus \{0\}$  as the unique solution (solution  $(\theta, \lambda) \in R_n \times [0, \infty)$  of the system possessing zero value when  $\varphi = 0$  or  $\lambda(\varphi, \varphi') = 0$  setting the integrands to zero with:  $H(x, \theta) = 0, H_\theta(x, \theta) = \lambda y, \lambda \geq 0$  where the lower bounds for  $S(\varphi)$  is directly achieved:

$$S(\varphi) = \inf_{\tau > 0} \inf_{\psi \in C_{x_1(0, \tau)}^{x_2} S_T(\psi)} \geq \int_0^1 \sup_{\theta: [0, 1] \rightarrow H(\varphi, \theta)=0} < \varphi', \theta > d\alpha \geq \int_0^1 < \varphi', \theta(\varphi, \varphi') > d\alpha$$

utilizing the first equation of the four. Furthermore,  $S(\varphi)$ 's upper bound can also be obtained through defining a minimizing sequences  $(T_k, \psi_k), k \in \mathbb{N}$  with the following rescaling process: For every  $k \in \mathbb{N}$  let:  $\lambda_k(\alpha) = \max(\lambda(\varphi(\alpha), \varphi'(\alpha)), 1/k), \alpha \in [0, 1], B_k(\alpha) = d\alpha, \alpha \in [0, 1], T_k(\alpha) = B_k^{-1}(1), B_k(t) = \varphi(B_k^{-1}(t)), t \in [0, T_k]$  Specifically, the inverse of  $B_k$  is approximated with the Brownian standard  $\sigma x$  satisfying the  $\alpha(0) = \lambda_k(\alpha(t))$  and thus  $1/k \leq \alpha'(t) \leq |\lambda_k|$  holds for all  $t \in [0, T_k]$  with the absolute continuity of  $\alpha(t)$ . And thus, the  $\psi_k$  is continuous in the whole time sequence  $(0, T_k)$ , enabling the inverse process:  $t = t(\alpha) = G_k(\alpha)$  with  $dt = d\alpha/\lambda_k$  and  $\varphi'(\alpha) = \psi_k'(t)G_k'(\alpha) = \psi_k'(t)/\lambda_k(\alpha)$ .

$$\text{Thus, } S_T(\psi) = \int_0^{T_k} L(\varphi, \varphi \lambda_k') / \lambda_k d\alpha$$

leading to the upper bound switching the integrate and limitation with  $k \rightarrow \infty$ , and with the proof in appendix B (in another work with landscape model) fulfilling the first order and second order conditions:  $\varphi' = H_\theta(\varphi, \theta)/\lambda$  is negative definite during the  $\theta$  maximizing process:  $L(\varphi, \lambda\varphi)/\lambda = \sup_{\theta \in R_n} (< \varphi', \theta > - H(\varphi, \theta)/\lambda)$  and guaranteeing them both fulfilled by  $\theta = \theta(\varphi, \varphi')$  with the

second equation, so that upper bound here is the same as the integrands of the lower bound as well as holds the  $\theta = 0$  when the  $\lambda = 0$  is satisfied, and therefore:

$$\frac{L(\varphi, \varphi \lambda'_k)}{\lambda} = \langle \varphi', \theta \rangle \geq -\frac{H(\varphi, \theta)}{\lambda} = \langle \varphi_0, \theta \rangle,$$

$$\theta = \theta(\varphi, \varphi')$$

The calculation can be found completely in Appendix B.

## 2.2. Diffusion approximation with numerical methods on the convert ratio referencing bacteria sensing and MTS on difference mapping

As to study the switching model interpreting the process explicitly, we thus combine the deterministic[15] background of the switching between on and off and give out one stochastic model based on the explicit (ordinary differential equation) ODE of the numbers of mRNA and proteins. Although the final model( referencing the quorum sensing model of bacteria in changing environment[16]) removes the dimers but it is used in the first place while cancelled out the in the quasi steady state according to its far more faster p roduction and degradation rate comparing to transcription and translation.(Simplified mechanism sees Figure 1). Start from the bistability of the metastability[17] of the two state model, with the absorbing boundary conditions,  $p_0(x^*, t) = 0$  and the identification of mean transition rate with principal eigen value  $\lambda_0 \varepsilon$ , the quasi-stationary approximation of

$$\rho_n(x, t) = C_0 * \exp(-\lambda^0 t) \varphi \varepsilon^0(x, n)$$

Furthermore, with the quasi-potential satisfying:

$$\sum_{n \in \mathbb{N}_0} S_n(x) (A_n, m(x) + \varphi'(x) \delta n, m) F_m(x) = 0,$$

$$H = 0.5(g_x^2 p_x^2 + g_x^2 p_x^2) + p_1 \varphi_1 + p_2 \varphi_2$$

where  $p_i$  is the momentum conjugate to the generalized coordinate  $x_i$ , where  $g_i = \sqrt{(S_{22} f_i + X_i / \tau_i)}$  (For more specific study of the  $\varphi_1$  and  $\varphi_2$  as the interacted diffusive speed, most studies applies WKB equations.) Since we focus on the transform between two status of the two populations, mRNA (of HS-1)  $X_n$  and proteins Hax1  $Y_n$  as the system.(with dimer Z of production rate  $k_{XY}$  and degradation rate  $k_P$ )[19] and the degradation rate of HS1 and hax1, as  $K_X$  and  $K_Y$ , separately. From the original ODES:

$$\frac{dZ}{dt} = k_{XY} XY - k_Z Z$$

$$\frac{dX}{dt} = -k_{XY} XY + k_Z Z = k_X X + \frac{V_Z * Z}{k_X + Z}$$

$$\frac{dY}{dt} = -k_{XY} XY + k_Z Z = k_X X + \frac{V_Z * Z}{k_X + Z} + \frac{V_Y * Z}{k_X + Z} + X_0$$

where  $X_0$  and  $Y_0$  are the initial volumes or baseline volumes of these two populations and with instant volume as  $V_X$  and  $V_Y$  and due to the zero value of  $dP/dt$ , the term of  $P$  can be replaced through:

$$P = -\frac{K_{XY}}{K_P} * XY$$

$$\frac{dX}{dt} = -\frac{K_X X}{1} + \frac{V_X}{1 + K_X K_P / K_{XY}} + X_0$$

$$\frac{dY}{dt} = -\frac{K_Y Y}{1} + \frac{V_Y}{1 + K_Y K_P / K_{XY}} + Y_0$$

Considering the transform of  $X$  (Upstream only), in the first step as degradation as the first term of right of the upper formula, the degradation part of  $X$  with  $k_X X$  which can be interpreted as the

Poisson process and rewrite into  $-\mu_1/\exp(P_x)$ , and in the second term, the coefficient of degradation part of  $X$ ,  $C_1$  is denoted as  $V_X * K_X/\mu_1$ . Meanwhile with the assumption of continuous Markov chain, where the convert ratio of  $Y$  is  $n$ , the  $k_{XY} * X * Y$  is equivalent to  $(Y/(X+Y))^n$  so that the whole degradation part becomes  $C_1\mu_1/(1+(y/(x+y))^n)\exp(P_x)$ ,  $C_2\mu_2/(1+(x/(x+y))^n)\exp(P_y)$ , and the final transform rate of mRNA number  $X$  and proteins  $Y$  are:  $C_1/(1+(y/(x+y))^n)(\exp(P_x) - 1) - \mu_1 X(\exp(-P_x) - 1)$  and  $C_2/(1+(x/(x+y))^n)(\exp(P_y) - 1) - \mu_2 Y(\exp(-P_y) - 1)$ , where the coefficient of degradation part of  $Y$   $C_2$  denoted as  $V_Y * K_Y/\mu_2$  as the reciprocal of the other population ratio. And as  $Y$  stands for the number of the proteins,  $X$  for the number of the mRNA separately with  $m$  and  $n$  as their translation and transcription rate. With the total sum of the system molecule numbers assumed as  $X+Y$ , we have the Hamiltonian:  $C_1/(1+(y/(x+y))^n)(\exp(P_x) - 1) - \mu_1 X(\exp(-P_x) - 1) + C_2/(1+(x/(x+y))^n)(\exp(P_y) - 1) - \mu_2 Y(\exp(-P_y) - 1)$ , where  $P_x, P_y$  are calculated setting  $H = 0$  and  $H_0 = 0$ , and conversion rate which can be calculated as  $dy/dx$ , specifically here, letting the first term equals the second and third equals the fourth term. (Complete see Appendix B) Note that: each single DNA population (hax1 and HS 1) has its own degradation rate when considering about its mRNA computation, and the other population's protein is taken as the intake, promoting its population when as normals binding onto the according site of persists, activating it. Vice versa, thus, the two populations have similar structured formula describing each degradation and population under the dual interacted population. The mean switching time is calculated based on the solution of the SDE:  $z' = z + \sqrt{(N_c/N)} \sqrt{1+2*\epsilon-z} * \eta$ , where  $N_c = 1/\tau$  and  $\eta N(0, \delta)$  is the white noise with correlator  $\langle \eta(\tau)\eta(\tau_0) \rangle = \delta(\tau-\tau_0)$ . Note that it is the span of the master equation in powers of the inverse population size  $N^{-1}$  re-scaling with  $\tau = 2^{(t/N)}$ , and  $z = x - 1 - x^2$  ranges over the interval  $[-1, 1]$  [20], leading to the solution  $\tau_0^* = 2\lambda/(1-2\lambda) \cot(\pi)$ . Thus, we have the algorithm:

\*\*\*\*\*

Input: maximum time scale size  $G$ , mRNA numbers  $y$ , proteins  $x$ , maximum steps  $Steps$ , tolerance  $Tol$ , parameters of the sensing model (coefficient of conversion  $c_1, c_2$ , transcription and translation rate  $m, n$ , degradation rate  $k_1, k_2$ , formation coefficients  $\mu_1, \mu_2$ , diffusion rate  $b_1, b_2$ ),  $dt$  as time increasement

Initilize: maximum time scale,  $T$ , maximum step number  $steps$ , tolerance  $Tol$ , numbers of mRNA after the first diffusion process that if necessary, initialized as one random the number, in the first status we start with the largest interval to cover higher possibilities, i.e.  $[x(0), x(0)+1, \dots, x[1]-1]$ ,

**for do**

$\hat{x}(\text{length}(\hat{x})) < x(i+1)$ : repeat

record the size  $T$ , time  $t$ , steps,  $Steps - steps + 1$

set the sequence according to size  $T$  (the interval for mRNA numbers)  $x(1), x(2), \dots, x(T)$  and generate the population number of proteins according data distribution,  $y(1), y(2), \dots, y(T)$ .  $T$  initialized as the  $X(i+1) - X(i)$ , consider Hamiltonian Markov (Hierarchical) [18]:

**if**  $\hat{x}$  exist (iterated from previous status) **then**:

segment the interval into several sub-sequences ( $X_0$  as the new current status,  $X_1$  as the previous status)

**end if**

**Note that:** As we only consider up streaming, down regulation into those before the previous status is not included.

**Function dynamics inputs:**  $x$  and fixed  $y$  (or  $x_0, y_0$ , or  $x_1, y_1$ )

Calculate degradation term w1 and w2 according to the (\*1)

Calculate px, py, dx, dy, conversion rate, He and Hx, s according to Appendix 2 predict multiplied mRNA and protein numbers xhat, yhat, and other Hamiltonians

Calculate update gamma, delta

Calculate tolerance for further stopping criteria as the residue of gamma and cell number with:

$$\begin{aligned} \text{tol} &= \text{abs}(\text{Gamma} - \text{gamma}) / \text{gamma}; \\ \text{toll} &= \text{mean}(\text{abs}(\text{xhat} - \text{x1}) / \text{x1} + \text{abs}(\text{yhat} - \text{y1}) / \text{y1}) \end{aligned}$$

**Output:** H, XHat, HthetaX, HthetaY, HxX, HxY, HamilX, HamilY, HamulXhat, HamilYhat, xhat, sX, sY, px, py, pxhat, pyhat, actionratio, delta, gamma, Delta, Gamma, cr1, c1, c2, crhat, c1hat, c2hat, tol, toll, Txc, Tyc, Txchat, Tychat

**Concatenate results:**

**If** X0, X1 exist then:

$$\text{Xhat} = [\text{X0hat}, \text{X1hat}];$$

**End if**

**If** only x0 exist then

$$\text{Xhat} = \text{X0hat};$$

**End if**

Do similar prediction regenerate the mRNA numbers X according to Y with

**Function dynamics** again for comparison. Results are with postfix 'L'

Store the quantities of 'successful' moves with smaller tolerance and action for either from mRNA or protein numbers.

**If** satisfies the configuration condition **then**

$$\text{Tol} = \min(\text{tol} + \text{toll}, \text{tol} + \text{tolL});$$

**Else**

Fail++

**End if**

## 2.3. Stochastic Model

### 2.3.1. Probabilistic Uncertainty Conditional

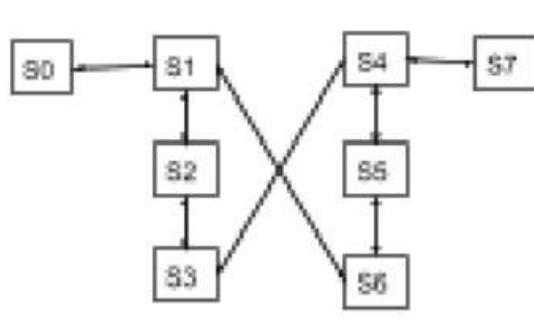


**Figure2: Belief Graph,**

Where S0 =  $\text{hax1\_DNA}^{\text{inactive}} \wedge \text{hax1\_DNA}^{\text{low\_concentration}}$

$S1 = \text{hax1\_DNA}^{\text{active}} \wedge \text{hax1\_DNA}^{\text{high\_concentration}}$   
 $S2 = \text{hax1\_mRNA} \wedge \neg \text{degrade}$   
 $S3 = \text{hax1\_protein} \wedge \neg \text{degrade}$   
 $S4 = \text{HS1\_DNA}^{\text{inactive}} \wedge \text{HS1\_DNA}^{\text{low\_concentration}}$   
 $S5 = \text{HS1\_mRNA}^{\text{active}} \wedge \text{HS1\_DNA}^{\text{high\_concentration}}$   
 $S6 = \text{HS1\_mRNA} \wedge \neg \text{degrade}$   
 $S7 = \text{HS1\_protein} \wedge \neg \text{degrade}$

Transition rate: R/P(R for CTMC, P for DTMC)

### 2.3.2. Model Check for Stochastic Models Combining Continuous Time Markov Chain with Embedding in Reward Computation

The logic applied on a probabilistic notion regards to the belief graph is based on the trust which is reflected by the reliability and predictability. Specifically, the language of the stochastic models used for computing CTMC is the Continuous Stochastic Logic(CSL) developed and extended by some research[20]

A CTMC is a tuple  $C = (S, s, R, L)$  where  $S$  is the finite set of states,  $s$  is the initial state ;  $R$  is  $S \times S \rightarrow R > 0$  is the transition rate matrix;  $L: S \rightarrow 2AP$  is a labelling function which assigns to each state  $s \in S$  is the set  $L(s)$  of atomic propositions valid in the state. Instead of the case of DTMCs, a fixed set of atomic propositions  $AP$  is applied, the transition rate matrix  $R$  assigns rates to each pair of states in the CTMC, used as parameters of the exponential distribution. A transition can only occur between states  $s$  and  $s'$  if  $R(s, s') > 0$ , representing the probability of this transition being triggered within  $t$  time-units equals  $1 - e^{-R(s, s')t}$ . Time spent in state  $s$ , before such transition occurs, is exponentially distributed with rate  $E(s)$ , where:  $E(s) = \sum(R(s, s'))$ , where  $E(s)$  is known as the exit rate of state  $s$ .

The embedded DTMC of a CTMC, is the probability of each state  $s'$  transitioned from the previous  $s$ , independent of the time, defined as:

$\text{Emb}(C) = (S, s, \text{Pemb}(C), L)$  where for  $s, s' \in S$ :

$$\text{Pemb}(C)(s, s') = \begin{cases} R(s, s') / E(s), & \text{if } E(s) \neq 0 \\ 1, & \text{if } E(s) = 0 \text{ and } s = s' \\ 0, & \text{otherwise} \end{cases}$$

where the behavior of the CTMC in the alternative way remains in a state  $s$  delayed and exponentially distributed with rate  $E(s)$  and transit with  $\text{Pemb}(C)(s, s')$ .

The infinitesimal generator matrix for the CTMC  $C=(S, s, R, L)$  is the matrix  $Q: S \times S \rightarrow R$  defined as:

$$Q(s, s') = R(s, s'), \text{ if } s \text{ is not } s' - \sum s'' \neq s, R(s, s') \text{ otherwise}$$

The CTMC stores the transition from  $s$  to  $s'$  in ratio format instead of the possibility in DTMC. However, the probability measures  $\text{Prs}$  on  $\sum \text{PathC}(s)$  as the unique measure such that  $\text{Prs}(C(s)) = 1$  and for any cylinder  $C(s, I, \dots, I_{n-1}, s_n, I', s')$ ,  $\text{Prs}(C(s, I, \dots, I_{n-1}, s_n, I', s'))$  equals:

$$\text{Prs}(C(s, I, \dots, I_{n-1}, s_n)) = \text{Prs}(C(s, I, \dots, I_{n-1}, s_n)) * \text{P1emb}(C1)(s_n, s') (e^{-E(s_n)} * \inf - e^{-E(s_n)} * \sup I')$$

In our case, such model check as with PCTL, we can easily derive the path formulae for the states between  $S0$  and  $S7$  separately with 6 time intervals  $I = [t_0, t_i]$  :

$$P \sim p[\Diamond I \varphi] = P \sim p[\text{true} \text{ UI } \varphi],$$

$P \sim p[\Diamond I \varphi] = P \sim p[\text{exist UI } \varphi]$ ,  $\varphi = \text{'transit'}$ , Stands for the probability that a transition occurs in time interval  $I=[t_0, t_i]$ , And thus, For determining the least solution,

$$\text{ProbC}(s, \varphi, I, U[0, t], \psi)$$

$$= \int \sum \text{Pemb}(C)(s, s') * E(s) * e^{-E(s) * x} * \text{ProbC}(s', \varphi, I, U[0, t], \psi)$$

$$= \text{ProbC}(\varphi, U[t, \infty]) = \text{Prob}\{\text{ProbC}(s, \varphi, U[0, t' - t], \psi), \text{ if } s = \varphi \text{ 0 otherwise}\}$$

And define the rewards function a CTMC  $D=(S, s, R, L)$ , the semantics is defined as:  $S \models R \sim r[I=t]$ ,  $\text{ExpC}(s, XI=t) \sim r$

### 2.3.3. Model Check for Stochastic Models reachability/safety computing based on Discrete Time Markov Chain(DTMC) approximating the Discrete Time Markov Process(DTMP)

In the second application of model check, the continuous dynamics described by switching diffusions is studied with reachability and dually safety properties on DTMC. Compared with the MC on continuous time domain, DTMC is defined with a fixed, finite set of atomic







### 3.1. Finding three critical points and explore their stability

As we have data (see Appendix C) of 15 status in all both for hax1 and HS 1 with their different cell numbers taken as X and Y in our model. For reward computation for their Markov chain, we pre-compute the their Hamiltonians, Action Potentials, mean switching time and related dynamics in the form (see availability), and the 6upstreaming status, which is the focus of the experiment application of our model. Using the pre-computation results, we are able to discuss about some practical problems about the current model. There are three groups of quantities studied combining the action potential as well as Hamiltonian inspired by bacterial quorum sensing, 'momentum and cell numbers', 'MTS with the SDE', and 'corresponding Hamiltonians', of each transform status in Appendix A.

First, we use the Taylor expansion to simplify the four ODE achieved in Appendix B: to

$$dx = C1/(1+(y/(x+y))^m) \mu Px - \mu 1 * x * PX$$

$$dy = C2/(1+(x/(x+y))^n) \mu PY - \mu 2 * y * PY$$

$$dPx = C2m(x/(x+y))^{m-1}/(1+(x/(x+y))^m)^2 (PY-1) - \mu 1 * Px - \mu 1$$

$$dPY = C1n(y/(x+y))^{n-1}/(1+(y/(x+y))^n)^2 (Px-1) - \mu 2 * PY - \mu 2$$

Note that our model here simplify the origin model where  $C_i = a_i/b_i$ , with  $b_i = 1$  as the burst size of protein i,  $x/(x+y) = x/(K2*(x+y))$  as  $k2 = 1$  is the dissociation constants standing for gene x binding on y's protein binding site. Regarding x and y as leading order variable, we apply phase analysis to consider the solution's stability around the three zero-energy points, which achieved through setting dx, dy, dP X and dP Y all to zero and combine the Hamiltonian's special case when  $H = 0$  (and  $H P = 0$ ):  $P1(x, y, \mu 2 * X/C1, \mu 1 * Y/C2)$ , where x and y are the solution of  $x = C1\mu 1 * (1+(y/(x+y))^n)$  and  $y = C2\mu 2 * (1+(x/(x+y))^m)$ ,  $P2(x, y, 0, 0)$ , where x and y are the solution of  $x = C1\mu 1 * (1+(y/(x+y))^n) = -y = -C2\mu 1 * (1+(x/(x+y))^m)$ , and  $P3(0,0,0,0)$  As P X and P Y are either zero or formula can be replaced by x and y around those three convergence points. We here, consider the analysis on x and y as following: denote  $dx = f(x,y)$  and  $dy = g(x,y)$ , and the we try to find  $x^*$  and  $y^*$  satisfy the  $f(x,y) = 0$  and  $g(x,y) = 0$  as well as holding the zero-energy points for their momentum. Thus with approximation:  $dx = f_X(x^*, y^*)(x - x^*) + f_Y(x^*, y^*)(y - y^*)$ , and  $dy = g_X(x^*, y^*)(x - x^*) + g_Y(x^*, y^*)(y - y^*)$ . We have

$$A = \begin{pmatrix} f_X & f_Y \\ g_X & g_Y \end{pmatrix} = \begin{pmatrix} -\mu 1 Px & \frac{C2n \left[ \frac{y}{x+y} \right]^{n-1}}{\left( 1 + \left[ \frac{y}{x+y} \right]^n \right)^2} Px \\ -\mu 2 Py & \frac{C1m \left[ \frac{y}{x+y} \right]^{m-1}}{\left( 1 + \left[ \frac{y}{x+y} \right]^m \right)^2} Py \end{pmatrix}$$

Where there exists the  $a > 0$ ,  $b > 0$  for the eigenvalue  $\lambda$ :

$$\lambda^2 + a\lambda + b = 0 \quad (1)$$

$$a = -(f_X + g_Y) | (x^*, y^*) \quad (2)$$

$$b = |A| \quad (3)$$

so that point  $(x^*, y^*)$  is the convergence points. Thus, we discuss about the stability of the three points as following: we denote  $X = (1 + (x/(x+y))^m)$  and  $Y = (1 + (y/(x+y))^n)$ , compute the a and b as:

$$\begin{aligned}
&= \mu_1 * P_X + \frac{C_{2m} \left( \frac{x}{x+y} \right)^{m-1} y}{\left( \left( 1 + \frac{x}{x+y} \right)^n \right)^2} = |A| (x^*, y^*) \\
&= u_2 * P_X * P_Y * C_{1n} \left( \frac{\frac{y}{(x+y)^{n-1}}}{\left( 1 + \frac{y}{x+y} \right)^n} \right)^2 \\
&\quad - u_1 P_X P_Y C_{1m} (x/(x+y))^{(m-1)/(1+x/(x+y))^n} n^2 \\
[1] \text{ for } P_1 \left( x, y, \mu \frac{2x}{C_1}, \mu_1 * P_X * P_Y * \frac{C_{2m} \left( \frac{x}{x+y} \right)^{m-1}}{\left( 1 + \frac{x}{x+y} \right)^n} \right), &\text{ where } x \text{ and } y \text{ are the solution of } x = C_1/u_1(1 + (y/(x+y))^n) \text{ and} \\
y = C_2/u_2(1 + (x/(x+y))^m), & \\
a = \mu_1 * u_2 * \frac{x}{C_1} + \mu_1 * y * \frac{C_{2m} \left( \frac{x}{x+y} \right)^{m-1}}{\left( \left( 1 + \frac{x}{x+y} \right)^n \right)^2} & \\
= \mu_2^2 * B^2 + \mu_1 * C_2 * A * m * (x/(x+y))^{(m-1)/\mu_2} / \mu_2 * A * B, &
\end{aligned}$$

[2] Thus, for P2,  $a = b = 0$ . It's unstable.

[3] for P3(0, 0, 0, 0), same as P2,  $a = b = 0$  and it's unstable.

### 3.2. HMC dynamics

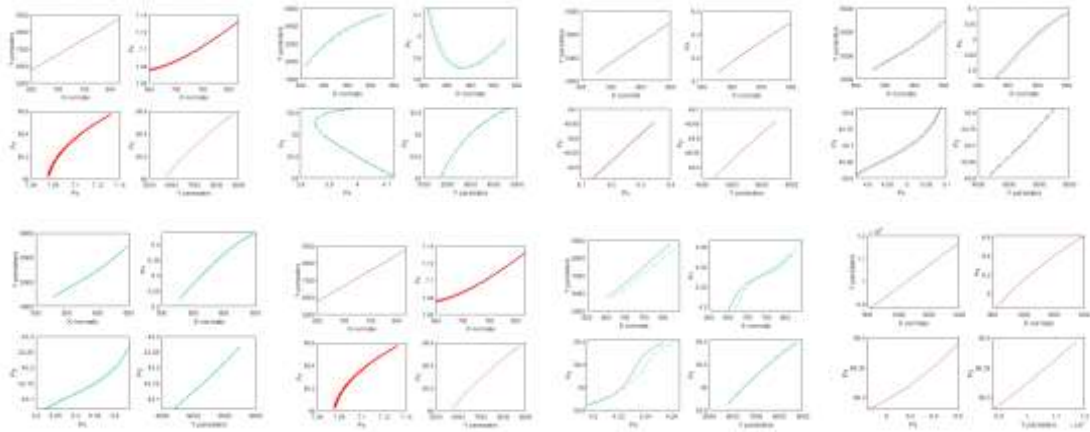


Figure 3(a)-(h) transition between mRNA and protein

In the second part here, with regard to the detailed behavior of mRNA and protein dynamics, we look into their momentum and numbers with 6 status (only the first 2(a)-2(c) and the last 2(d)-2(f) transition examples of the origin 3 groups \* 5 transition statuses figures) in all are studied detailedly while the whole data based on 15 status. As we only investigated the positive direction, the red ones (top left) the application on clinical data while green one (top right) in the larger scaled simulation with more transition status (blue dashed line is the predicted dynamics). Note that the persisters and normals are the roles they take in the whole process (considering from bifurcation to catastrophe and extinction) where here they can be all considered as promoters as their numbers both grows in this process until the last status as their interaction in constant environment is of our main interest as we mentioned before. Generally, with small change studied in one status, the trend is more significant than the larger scale transition. For instance, the green simulation are always more sensitive to the momentum change and shows them more significantly on the cell trajectory comparing to the red clinical transition (we manually break one clinical status into sub-status in simulations.)

Specifically, in the 1 → 2 transition, the production of the HS 1 is slightly faster than hax1 with the accelerate from faster to slower as well as the hax1 0 s momentum decreases from fast to slow while HS 0 1 s momentum increases from fast to slow similarly. The larger scaled

simulation show the trend similarly but with larger momentum difference and thus gives out the curve trajectory instead of straight line in the top left figure; On contrary, in  $2 \rightarrow 3$  transition, both the clinical application and larger simulation give totally the same behavior according to the dynamics, where proteins produce faster than mRNA but with similar acceleration. Other transition can be similarly analyzed. Note that from the  $4 \rightarrow 5$  of the larger scale simulation, there starts to show the switching where the protein changes into persistence with degradation instead of production which can be both detected from cell numbers figure in the top left and momentum figures in the right bottom although the fewer status contained clinical data does not show this behavior yet. In the last transition status, the switching of proteins becoming into persistence is detected in both clinical process and simulation, where in the clinical data, the momentum change of proteins and mRNA are both linear process while in simulation, the momentum of the mRNA grows slightly from faster to slower and proteins degrade slightly from faster to slower as well and in the last short time, proteins go back to normal again which according to the rising number change in the top left and increase in the momentum both relatively to mRNA (left bottom) and absolutely (right bottom.)

In the second series of figures 2(c), 2(f), we compute the mean time to switch approximation with the solution based on mapping to their difference space where we choose the object as 1) single population of mRNA to the end of the transition (top left); 2) single population of proteins to the end of the transition (top right); 3) mRNA population to the end status of protein (left bottom) and 4) proteins population to the end status of mRNA (right bottom). There gives some different patterns, as in the  $1 \rightarrow 2$ , both the mRNA and proteins have the mean time to switch increase linearly with their number change while there exists one significantly longer time at 0.4 for the proteins compared to the final status of mRNA and one totally unstable transition recorded; In the  $2 \rightarrow 3$ , all the MTS increase linearly with the cell number growth; In the  $4 \rightarrow 5$ , as there exists the decrease of proteins thus there exists one negative MTS stands for the status; And in  $5 \rightarrow 6$ , the last status for the proteins again, compared to the final status where the number back to increase, the previous degradation status also leads to the minus MTS but positive to the mRNA as they both grow in the end. In the last part, Further application using the transition matrix of the model, we compute some basic Markov chain quantities based on the stochastic process as following with the pre-computation result (in availability):

The first step of the further computation of rewards of continuous Markov Chain is to prepare the matrix as follows: use conversion rate computed as transition rate in matrix R:  $R =$

$$R = \begin{bmatrix} 0 & \text{ConvertRate1} & 0 & 0 & \text{ConvertRate5} & 0 \\ \text{ConvertRateL1} & A & \text{ConvertRate2} & 0 & B & 0 \\ 0 & \text{ConvertRateL2} & 0 & \text{ConvertRate3} & 0 & 0 \\ 0 & 0 & \text{ConvertRateL3} & 0 & \text{ConvertRate4} & 0 \\ 0 & 0 & 0 & \text{ConvertRateL4} & 0 & \text{ConvertRate5} \\ 0 & 0 & 0 & 0 & 0 & 1 \end{bmatrix}$$

where  $A = \text{ConvertRate1:5}$ ;  $B = \text{ConvertRateL1:5}$ ; we have:  $R =$

$$\begin{bmatrix} 0 & 0.0095 & 0 & 0 & 0 & 0 \\ 0.9634 & 0 & 0.0015 & 0 & 0 & 0 \\ 0 & 0.0001 & 0 & 0.0005 & 0 & 0 \\ 0 & 0 & 0.0002 & 0 & 0.8678 & 0 \\ 0 & 0 & 0 & 0.0362 & 0 & 0.1207 \\ 0 & 0 & 0 & 0 & 0 & 1 \end{bmatrix}$$

Then, we get the approximated marginal distribution by summation of R:  $E = \text{sum}(R, 2)$ , and the embedded probability:  $P_{emb} = -\frac{R}{\text{repmat}(E', 6, 1)} + \text{diag}([E']) =$

$$\begin{bmatrix} 0.0095 & -0.9999 & 0 & 0 & -0.0001 & 0 \\ -0.9985 & 0.9649 & -0.0015 & 0 & 0 & 0 \\ 0 & -0.1658 & 0.0006 & -0.8680 & 0 & 0 \\ 0 & 0 & -0.0002 & 0.8680 & -0.9998 & 0 \\ 0 & 0 & 0 & -0.2309 & 0.1570 & -0.7691 \\ 0 & 0 & 0 & 0 & 0 & 0 \end{bmatrix}$$

$$Q = R + \text{diag}([E']) = \begin{bmatrix} 0.0095 & 0.0095 & 0 & 0 & 0 & 0 \\ 0.9634 & 0.9649 & 0.0015 & 0 & 0 & 0 \\ 0 & 0.0001 & 0.0006 & 0.0005 & 0 & 0 \\ 0 & 0 & 0.0002 & 0.8680 & 0.8678 & 0 \\ 0 & 0 & 0 & 0.0362 & 0.1570 & 0.1207 \\ 0 & 0 & 0 & 0 & 0 & 2 \end{bmatrix}$$

$$P_{unif} = \text{eye}(\text{size}(Q)) + \frac{Q}{\max(E)} = \begin{bmatrix} 1.0095 & 0.0095 & 0 & 0 & 0 & 0 \\ 0.9634 & 1.9649 & 0.0015 & 0 & 0 & 0 \\ 0 & 0.0001 & 1.0006 & 0.0005 & 0 & 0 \\ 0 & 0 & 0.0002 & 1.8680 & 0.8678 & 0 \\ 0 & 0 & 0 & 0.0362 & 1.1570 & 0.1207 \\ 0 & 0 & 0 & 0 & 0 & 3 \end{bmatrix}$$

1) taking  $I0 = [0, 2]$ , from 0 to 54:

$$\text{Prob} = P_{emb}(1, 5) * (\exp(-E(1)*0) - \exp(-E(1)*4)) = [0.0095, 0.9649, 0.0006, 0.8680, 0.1570, 1];$$

2)  $\text{Prob}(\text{trueU}[0, 2], s4) : \text{stat} = \max(E) * 2$

$n = 4;$

$\text{Probc} = 0$

FOR:  $i = 1 : n$

$$\text{Probc} = \text{Probc} + \exp\left(\frac{(-\text{stat}) * \text{stat}^i}{\text{factorial}(i)}\right)$$

END

$$\text{Probc} = \text{Probc} * [0, 0, 0, 0, 1, 0]' = [0, 0, 0, 0, 0.8120, 0];$$

3) The number of cells expected after 6 time units have inactivated can be given by

$$\text{Exp}^C(s, X_c \leq t) = \frac{1}{q} * \sum_{j=0}^{\infty} \exp(-qt^j) * \frac{(qt^j)^j}{\text{factorial}(j)} * (P_{unif})^j * (q * P_{unif} * [1, 1, 1, 1, 1, 1])'$$

$$\text{Probc2} = 1.0e+03 * \begin{bmatrix} 0.0487 & 0.0024 & 0 & 0 & 0 & 0 \\ 0.2475 & 0.2941 & 0.0004 & 0 & 0 & 0 \\ 0 & 0.0000 & 0.0464 & 0.000 & 0 & 0.0001 \\ 0 & 0.0001 & 0.0000 & 0.2555 & 0.2258 & 0.0393 \\ 0 & 0 & 0 & 0.0094 & 0.0704 & 0.0827 \\ 0 & 0 & 0 & 0 & 0 & 1.3212 \end{bmatrix}$$

$$\text{Probc2} = 1.0e+03 * [0.0526, 0.6184, 0.0471, 0.6051, 0.1983, 1.8000];$$

Thus, if we want to know: the status when after 6 unit times products mRNA cells over 1000 the only satisfied status is the last one which might product 1800 mRNAs.

Figure 4 computation of probabilistic safety

In the probabilistic safety computation by finite DTMC abstraction, the computation is based on the differential cognitive (\*) in 2.3.3 with the previous unified matrix of CTMC composed of 6 transition status and 6 time points for each,  $dX = P(:, 2:6) = P(:, 1:5);$

Continue the error bounds for time discretization in 2.3.3, considering mean:  $\text{Mu} = \text{mean}(P, 1);$

$\text{Sigma2} = \text{var}(P, 1); \text{Sigma} =$

$\text{std}(P, 1); W \sim N(\text{Mu}, \text{Sigma2}) = \text{repmat}(\text{ones}(1, 6) ./ \sqrt{2 * \pi * \text{Sigma2}}, 6, 1) * \exp(-P -$

$\text{repmat}(\text{Mu}, 6, 1) ./ 2 ./ \text{repmat}(\text{Sigma} ./ 2, 6, 1);$  Then the Brownian,  $G = \exp(\text{Mu} * t -$

$\text{Sigma} ./ 2 * t + \text{Sigma} * W);$

With  $d = \sqrt{((X)^2)}$ ,

As  $dt = 1$  fixed,  $Kd = \max(d) = 1.3433;$  And with sampling time  $h = \min(2(-6)/2/\sqrt{(2)/K2/Kd}, 2(-6)) = 0.28558$

Finally, with  $I = 0:5, Pds = T, z0 = 1,$  we can achieve:

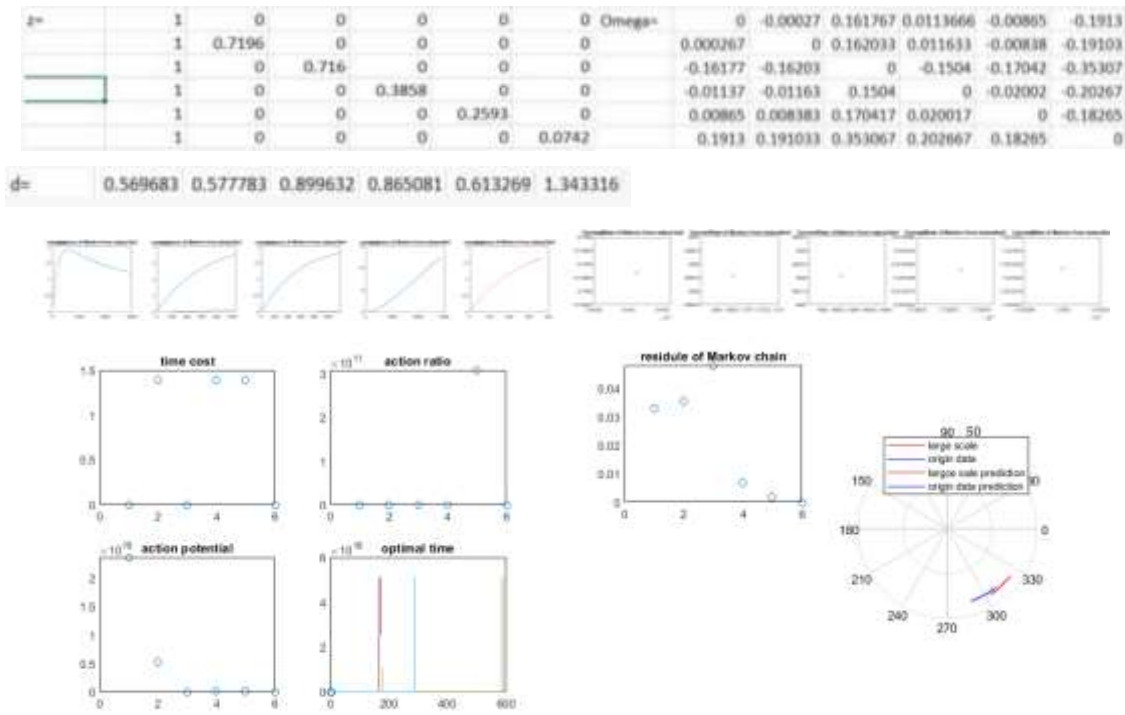


Figure 5. (i) convergence of MC; (j) convert rate from low I to i+1 level (k) total metrics related to time domain; (l) residue of Markov Chain and phase.

## IV. CONCLUSION

In general, Hamiltonian markov chain advantage over the markov chain random walk with its faster convergence. As in 2(i) and 2(j), the convergence (variation to mean) of the markov chain hamilton is in blue line and the red line for clinical data and simulation on more possible transition status, giving different convergence but similar phase interval (according to 2(k)), interestingly. The last status transition converge the worst followed by the first transition. And the result simulated with more markov chain status converges better than the clinical results. And according to the convert rate, the mRNA to Protein transfer ratio should be the highest when starting, and goes especially lower in the last two status which is in assistance to the protein binding as we cut off the process around the convergence point where the two population has reached metastability  $F_M$ . According to the simulation result, the protein has gone through the switching process changing from normals to persisters and back to normals (bursts in optimal time in 2(j) might also due to the switch.).

Mean while, as the second population providing food (protein) to the other's binding site and either activate or deactivate it, it works as the extrinsic noise induced the excitability or exhibition of the other gene. Here, as we choose *hax1* and *HS 1*, they work as promoters for each others. One noticeable computation is the reward computation based on stochastic model selection which is useful in predict the possible status of the cell numbers easily with precomputation. And we can consider correct the transition matrix with simulated clinical tested results to improve the prediction as well. On the other hand, the most important calculation action potential is easier to be achieved through Hamilton as we proved with geometric minimum action and stochastic approximation. Other methods can cover Hamilton Jacobian matrix, WKB and etc. As we also improve the algorithm with adding hierarchical markov in calculating number of cells in different status only record successful move according to the tolerance based on action potential and residual of prediction numbers both, the convergence of the algorithm is guaranteed. And further research can be conducted on the whole process from bifurcation to catastrophe and extinction as well. Problem with multi population is also possible. As *hax1* is observed to have function in signaling and regulating of genes especially in learning

systems and motor related brain function, this switching model study related to its binding might help to predict the cell numbers and production or degradation rate especially later with further study into both with promoters and persisters as to test different drug and their efficiency on the aging process related disease.

In the computation of reachability, the approximation with DTMC mainly compute the kernels of Brownian with shift, finally discretize the original switching diffusion process. As the DTMC gives out the kernel with probability instead of the ratio, it is then convenient to be written into transition matrix  $P_{dx}$  which is discretized from  $S_{dx}$  on finite space state and gives out the reachability with error  $I/h*(K_{dx}+\exp(-2^n-2^{n/2+1}))$ .

As the proof in Appendix, the error bounds with Lipschitz constants converged with prominent  $K = mh_1 + Lh_2$ . And the computed result  $N*K*dx$  is here is 0.453 with  $N = 6$ ,  $m = L = 2$ ,  $dx = 0.002$  and  $h_1 = 0.001$ , and  $h_2 = \text{ceil}(h_2*N) = 1.71$ .

Since the final result of the continuous process is not of probability range thus we normalize it with  $P = \text{ratio}/\text{sum}(\text{ratio})$  and the DTMC approximation shown in the figure is the approachability(1-safety.) The result of the ttest tested continuous embedded matrix and  $h = 0$ ,  $p = -0.0515$ ,  $ci = -0.7212$ ,  $0.0029$ ,  $\text{stats} = \text{struct with stat: } -2.2103$  (df: 10), do not reject the hypothesis that the two process. As the final safety consistently for two methods gives highest concentration for the last state showing the example computation's direction from off to on, although there is the slight difference that the forth in the continuous process is relative lower comparing to its other five states as well as the one in the discrete process states. The DTMC gives strictly increasing concentration from off to on during the 6 states. switching diffusion is a commonly used model in genetic field, not only useful in the transmission of different molecules but also can be derived into analytical models giving straight transfer information about some process with either concentration change or energy change.

## ACKNOWLEDGEMENTS

Although I have graduated with excellence graduates awards, I am still working in the university currently cooperated with university hospital. Thanks to all the supervisors and colleagues I have worked with.

## REFERENCES

- [1] Freedman, H.I., Dynamics of simple gene-network motifs subject to extrinsic fluctuations, 1980
- [2] Noufe H. Aljahdaly, Analytical Solutions of a Modified Predator-Prey Model through a New Ecological Interaction, 2019 [ensembl](https://www.ensembl.org/index.html), <https://www.ensembl.org/index.html>
- [3] Ingo Lohmar, Baruch Meerson, Switching between phenotypes and population extinction, Racah Institute of Physics, 2018
- [4] Marta Kwiatkowska, Gethin Norman, David Parker, Stochastic Model Checking, Oxford, 2019
- [5] David Martínez-Rubio, Varun Kanade, Patrick Rebeschini, Decentralized Cooperative Stochastic Bandits, Oxford, 2005 Paul C Bressloff, Stochastic switching in biology: from genotype to phenotype, Department of Mathematics, University of Utah, 2017 Baier, Christel, Principles of Model checking, Massachusetts Institute of Technology, 2008
- [6] Cheng Lv, Xiaoguang Li, Fangting Li, Tiejun Li, Constructing the Energy Landscape for Genetic Switching System Driven by Intrinsic Noise, Peking University, 2014
- [7] C.W. Gardiner, Handbook of Stochastic Methods for Physics, Chemistry and the Natural Sciences, 4th ed., Handbook of Stochastic Methods for Physics, Chemistry and the Natural Sciences, 4th ed., Springer, 2009 Alberto Finzi, Thomas Lukasiewicz, Game-Theoretic Agent Programming in Golog Luca Cardelli, Marta Kwiatkowska, Robustness Guarantee. Yasar Demirel, in Non-equilibrium Thermodynamics (Third Edition), 2014
- [8] Matthias Heymann, Eric Vanden-Eijnden, Geometric Minimum Action Method: A Least Action Principle on the Space of Curves, Courant Institute, 2007

- [9] Approximate Model Checking of Stochastic Hybrid Systems: Alessandro Abate, Joost-Pieter Katoen, John Lygeros, Maria Prandini. Marta Kwiatkowska, Gethin Norman, Stochastics Model Checking
- [10] An experimental investigation on the health monitoring of concrete structures using piezoelectric transducers at various environmental temperatures.
- [11] Author Robert Balson Dingle, Their Derivation and Interpretation, Academic Press, 1973 J.C., Gittins, Keble College, Oxford, 2010
- [12] Ali, Isra, Alfarouk, Khalid O., Reshkin, Stephan J., Ibrahim, Muntaser E., Doxycy-cline as Potential Anti-cancer Agent, Anti Cancer Agents, 2018
- [13] G.S. Skone, Irina Voiculescu, Stratagems for effective function evaluation in computational chemistry, Oxford, 2010
- [14] Zahid Ur Rehman, Quorum-Quenching Bacteria Isolated From Red Sea Sediments Reduce Biofilm Formation, KAUST,2016
- [15] Peter Minary, Charlotte M Deane, Explorong peptide/MHC detachment process using hiearchical natural move Monte Carlo, Oxford, 2015Biancalani, E. Giamperi, A. Bazzani, G. Catellani, and A. M aritan, Phys.Soc, Jpn., Physics, 2015
- [16] D.M. Roma, R.A. P'Flanagan, A.E. Ruckenstein, A.M. Sengupta, R., Optimal path to epigenetic switching, Rarah Institute of Physics,2015 C HASTE : incorporating a novel multi-scale spatial and temporal algorithm into a llarge-scale open source librarty B Y M IGUEL O. B ERNABEU 1 , R AFEL B ORDAS 1 , P RAS P ATHMANATHAN 1 , J OE P ITT -F RANCIS 1 , J ONATHAN C OOPER 1 , A LAN G ARNY 2 , D AVIDJ. G AVAGHAN 1 , B LANCA R ODRIGUEZ 1 , J AMES A. S OUTHERN 1,3 AND J ONATHAN P. W HITELEY 1, \*
- [17] Chris Holmes Leonhard Held Bayesian Ausiliary Variable Models for Binary and Multinomiak Regression
- [18] Michael Betancourt and Mark Girolami Hamiltonian Monte Carlo for Hierarchical Model
- [19] rffany Amariuta, Ynag luo, Steven Gazal, Emma E. Davenport, Bryce van de Geijn, Kazuyoshi Ishigaki, Alkes L. Price, IMPACT: Genomic Annotation of Cell-State-Specific Regulatory Elements Inferred from the Epigenome of Bound Transcription Factors.
- [20] Dynamics statistic Markov chain, Alessandro Abate, Joost-Pieter Katoen, Alexandru Mereacrem

## AUTHORS



Qin He

Received master degree in data engineering and machine learning with physics minor. During Bachelor(Maths bachelor in ECUST, student union technology and entrepreneur department academic division leader,minor in English), did research study in dynamics neuron networks lab, using statistics, data mining basic skills. Minor in English. In currently master program, doing neuroscience research study related to neuro imaging, neuron computation, minoring in Physics.) Main field in Mathematics and programming, with equal interest in other natural science and technology.

And due to past background in machine learning with disciplinary projects, especially related to biomedical and neuroscience in processing time series, frequency spectrums and Bayes models combining stochastic process, computational modeling with python, matlab, C/C++ and a little bit C#, I would really like to have intern in developing and algorithms of ML.



Rubin Wang

Received the Ph.D. degree in electronic and mechanical engineering from Nagoya University, Nagoya, Japan, in 1998.,He is currently one of the Director of the Institute of Cognitive Neurodynamics, East China University of Science and Technology, Shanghai, China. His research interests are in the areas of cognitive neurodynamics, coding and decoding theory in brain information processing, complexity theory, analysis of biological neural networks, and computational vision and audition.,Dr. Wang serves as the founding Editor-in-Chief of Cognitive Neurodynamics.



Xiaochuan Pan

Received the Ph.D. degree in biophysics, University of Chinese Academy of Sciences, in 1997.,He is currently one of the Director of the Institute of Cognitive Neurodynamics, East China University of Science and Technology, Shanghai, China. His research interests are in the areas of cognitive neurodynamics, coding and decoding theory in brain information processing, complexity theory, analysis of biological neural networks, and computational vision and audition.Dt.Pan is professional at behaviour models related to deduction, conditional random dynamics and optimization.



## Appendix

A Please find supplementary data, code and experimental results in this link:  
<https://github.com/dashboard>

## B Proof

As our assumption of diffusion process is based on the proposition of the geometric quasi-potential:

$$V(x_1, x_2) = 2 * \inf \int_T |h|_x \sin^2(\frac{1}{2}) \eta ds$$

which later can be used in computing quasi-potential under the case without SDE:

$$V(x_1, x_2) = \inf_{\phi \in C^2([0,1])} S(\phi) \text{ with } S(\phi) = \sup_{\theta \in [0,1] \rightarrow \theta'' \in \mathbb{R}^n} \int_0^1 \langle \phi', \theta \rangle d\alpha \text{ As we have}$$

proved the most important invariance of the key four representation of the action through the same value of upper bound and lower bound of S. The only supplementary required is after the rewrite of  $V(x_1, x_2)$  with S, the inf is computed with the lower-semicontinuity of S and the compactness of certain functions: Consider the times  $\theta_k \in C_{\theta_k}([0,1])$  satisfies the  $T_k$  and  $\psi_k$  such that with some normalized unit speed  $(\theta_k') = L_k([0,1])$  they

through the curves and the  $L_k$  is the length of the curve  $\psi_k$ . On  $[0, T_k] \rightarrow [0,1]$ ,  $\alpha_k$  is defined as  $(\frac{1}{L_k}) \int_0^{\alpha_k} |\psi_k'(t)| dt$

$L_k = \int_0^{T_k} |\psi_k'(t)| dt$  and with inverse as  $u(t) \in [0,1]$   $\alpha_k(u) = u$ , and the set  $\alpha_k(\psi_k(t)) = \psi_k(t)$  for all  $t \in [0, T_k]$  both  $\alpha_k' = \frac{|\psi_k'|}{L_k}$  and  $L_k = |\psi'| = \frac{|\psi_k'|}{\alpha_k'} \alpha_k' = |\psi'|$  so that  $\psi_k = \psi$ , i.e.,  $\psi_k \in C_{\theta_k}([0, T_k])$ . With the first equation of the

four we proved, we have the estimate of S as:  $\inf_{\phi \in C_{\theta_k}^2([0,1])} S(\phi) \leq S(\theta_k) = \inf_{\psi \in C_{\theta_k}([0,T])} \int_T \langle \psi', \psi \rangle dt \leq \int_{T_k} \langle \psi_k', \psi_k \rangle dt$  where when  $k \rightarrow \infty$ , the right-hand side converges to the left-hand side, and it follows that

$$\lim_{k \rightarrow \infty} S(\theta_k) = \inf_{\phi \in C_{\theta}^2([0,1])} S(\phi)$$

With  $M = \sup_k \langle \psi_k', \psi_k \rangle = \sup_k L_k < \infty$ , and thus  $\theta_k$  that converges uniformly to one limiting function  $\theta \in C_{\theta}([0,1])$  we have:

$$S(\theta) = \inf_{\phi \in C_{\theta}^2([0,1])} S(\phi)$$

and thus  $\theta$  is a minimizer of S. Since the functions  $\theta_k$  are time-truncated  $\theta_k$  and converge uniformly to  $\theta$ , by the

$$\rho(\theta_k, \theta) = \rho(\theta_k, \theta) \leq \rho(\theta_k, \theta) \leq \rho(\theta_k, \theta) \rightarrow 0 \text{ as } k \rightarrow \infty$$

In addition, with the minimizer of S unique to reparametrization and let  $\theta$  be the limit of some converging subsequence of  $\langle \psi_k', \psi_k \rangle$  from the assumption that  $\rho(\theta_k, \theta) \rightarrow 0$  as  $k \rightarrow \infty$  and with  $\theta_k \in C_{\theta_k}([0,T_k])$  that converges in Frechet metric to some limit  $\theta$  is a minimizer of S. And thus,  $\rho(\theta) = \rho(\theta_k)$  where  $\rho(\theta_k) = \rho(\theta_k, \theta) \rightarrow 0$  as  $k \rightarrow \infty$  which contradicts. Some basic quantities of Hamiltonians: From our model after the Hamiltonian as follows:

$$\frac{C_1}{1 + (\frac{C_1}{C_2})^2} (exp(P_Y - 1) - \mu_1 + \mu_2 (exp(-P_Y - 1)) - \mu_2 + \mu_1 (exp(-P_Y - 1)) \text{ we calculate} \\ H_X, H_Y, H_{P_X}, H_{P_Y}, P_X, P_Y, H_X, H_Y, H_X = \mu_1 + (exp(-P_X - 1)) - \frac{C_2 \mu_1 (\frac{C_1}{C_2})^2 \mu_1 - 1}{(1 + (\frac{C_1}{C_2})^2) \mu_1^2} (exp(P_Y - 1)) \\ H_Y = \mu_2 + (exp(-P_Y - 1)) - \frac{C_1 \mu_2 (\frac{C_1}{C_2})^2 \mu_2 - 1}{(1 + (\frac{C_1}{C_2})^2) \mu_2^2} (exp(P_X - 1)) \quad H_{P_X} = \frac{C_1}{1 + (\frac{C_1}{C_2})^2} \mu_1 exp(P_Y - 1) + \mu_2 + \mu_1 (exp(-P_Y - 1)) \\ H_{P_Y} = \frac{C_2}{1 + (\frac{C_1}{C_2})^2} \mu_2 exp(P_X - 1) + \mu_2 + \mu_2 (exp(-P_X - 1)) \quad H_X = \frac{C_1}{1 + (\frac{C_1}{C_2})^2} \mu_1 (exp(P_Y - 1) + \mu_1 + \mu_2 (exp(-P_Y - 1)) \\ H_Y = \frac{C_2}{1 + (\frac{C_1}{C_2})^2} \mu_2 (exp(P_X - 1) + \mu_2 + \mu_1 (exp(-P_X - 1)) \quad dP_X = \frac{C_2 \mu_1 (\frac{C_1}{C_2})^2 \mu_1 - 1}{(1 + (\frac{C_1}{C_2})^2) \mu_1^2} (exp(P_Y - 1) + \mu_1 + \mu_2 (exp(-P_Y - 1)) - \mu_1 \\ dP_Y = \frac{C_1 \mu_2 (\frac{C_1}{C_2})^2 \mu_2 - 1}{(1 + (\frac{C_1}{C_2})^2) \mu_2^2} (exp(P_X - 1) + \mu_2 + \mu_2 (exp(-P_X - 1)) - \mu_2 \text{ Finally, because of the approximation with diff}$$

$$H_Y = \frac{C_2}{1 + (\frac{C_1}{C_2})^2} \mu_2 (exp(P_X - 1) + \mu_2 + \mu_1 (exp(-P_X - 1)) \quad dP_X = \frac{C_2 \mu_1 (\frac{C_1}{C_2})^2 \mu_1 - 1}{(1 + (\frac{C_1}{C_2})^2) \mu_1^2} (exp(P_Y - 1) + \mu_1 + \mu_2 (exp(-P_Y - 1)) - \mu_1 \\ dP_Y = \frac{C_1 \mu_2 (\frac{C_1}{C_2})^2 \mu_2 - 1}{(1 + (\frac{C_1}{C_2})^2) \mu_2^2} (exp(P_X - 1) + \mu_2 + \mu_2 (exp(-P_X - 1)) - \mu_2 \text{ Finally, because of the approximation with diff}$$

process [15], the Hamiltonian quantities are:  $H_{\theta_{\text{Hera}}}(a,b) = a(x) - 1 \{ \frac{b(x)}{a(x)} + \gamma - b(x) \}$   $\lambda(x,y) = \frac{b(x)}{a(x)}$  As a result,  $S(\theta)$  can be calculated explicitly with the Hamiltonian in a diffusive process as follows:

$$S(\theta) = \int_0^1 \langle \theta', \theta \rangle dt = \langle \theta', \theta \rangle dt > 0$$

### a.. linear regression method on data

Y = B\*X = -0.00114 -6.69764 1.11999 4345.69955 3.25582  
NA 0.33371

And the analysis summary :

#Coefficients: (1 not defined because of .66singularities)  
Estimate Std. Error t value Pr(>|t|)

(Intercept) -0.00114 0.060137 88 0.001425

as.matrix(X)V2 1.11999 0.003344 66.79 0.0001425 \*\*

as.matrix(X)V4 3.25582 0.000215 271.46 0.0001425 \*\*

as.matrix(X)V5 -0.44712 0.000600 1.02 0.0001425 \*\*

as.matrix(X)V6 0.33371 0.287314 2e10\*\*2 0.0001425 \*\*

Residual standard error: 0.231 on 456 degrees of freedom

Multiple R-squared: 1, Adjusted R-squared: 0.9946

F-statistic: 1.21e+02 on 2 and 456 DF, pvalue 254

The estimated effect of V2,V4, V5, V6 on the convert is 1.11999 3.25582 , -0.44712, 0.3371.

### b.Auxiliary method

to resampled the makorv transition matrix in the mRNA to protein switching model which is P1 before

1.0095	0.0095	0	0	0	0
0.9634	1.9649	0.0015	0	0	0
0	1.0000e-04	1.0006	5.0000e-04	0	0
0	0	2.0000e-04	1.8680	0.8678	0
0	0	0	0.0362	1.1570	0.1207
0	0	0	0	0	3

And Augmented into P2:

4.8461	2.0063	0	0	0	0
0.9379	0.6672	2.0242	0	0	0
0	2.0063	0.6836	4.2907	0	0
0	0	2.0242	2.3113	6.7428	0
0	0	0	4.2907	3.6798	2.5908
0	0	0	0	6.7428	1.1108

h=0 0 0 0 0 0

p=[0.3667, 0.4350,0.2222, 0.1495,0.1030, 0.8709]

ci=[ -2.2811,1.0108; -1.8172, 0.9155;-1.7683, 0.5251;

-3.7605, 0.7645; -5.7797, 0.7328; -1.5520, 1.3584]

And with those h all equals to 0, does not rejects the

P1 and P2 follows the same distribution.

## C.Code

```
MaxStep = 50;
W = eye(size(z));
X = z;
v = var(X)+0.000000001;
for steps = 1:MaxStep
temp = ones(size(v))./v;
Vtemp = inv(X'*inv(W)*X+temp);
V = Vtemp*eye(size(Vtemp))*Vtemp';
L = chol(abs(V),'lower');
S = V*X';
B = S*inv(W)*z;
% observations for normal with W
H = X*S';
CW = H./(W-H);
CW(isnan(CW))=0;
m = X*B;
m = m-CW.*(z-m);
qtemp = CW.*(CW+1);
qtemp(isnan(qtemp)) = 0;
% draw Z from truncated normal
q = sqrt(qtemp*eye(size(qtemp))*qtemp');
Z = X;
R = X;
%Z(:,i) = mvnpdf(X,mean(m,2)',q);
temp = mean(m,2)';
for i = 1:size(X,1)
Z(:,i) = normpdf(X(:,i),temp(i),q(i,i));
end
```

B.Auxiliary method to resampled the makorv transition matrix in the mRNA to protein switching model which is P1 before.

And Augmented into P2:

h=0 0 0 0 0 0

p=[0.3667, 0.4350,0.2222, 0.1495,0.1030, 0.8709]

ci=[ -2.2811,1.0108; -1.8172, 0.9155;-1.7683, 0.5251;

-3.7605, 0.7645; -5.7797, 0.7328; -1.5520, 1.3584]

And with those h all equals to 0, does not rejects the

P1 and P2 follows the same distribution.

A. linear regression method on data, (Y = B\*X) :

-0.00114 -6.69764 1.11999 4345.69955 3.25582

NA 0.33371

And the analysis summary :

#Coefficients: (1 not defined because of .66singularities)  
Estimate Std. Error t value Pr(>|t|)

(Intercept) -0.00114 0.060137 88 0.001425

as.matrix(X)V2 1.11999 0.003344 66.79 0.0001425 \*\*

as.matrix(X)V4 3.25582 0.000215 271.46 0.0001425 \*\*

as.matrix(X)V5 -0.44712 0.000600 1.02 0.0001425 \*\*

as.matrix(X)V6 0.33371 0.287314 2e10\*\*2 0.0001425 \*\*

Residual standard error: 0.231 on 456 degrees of freedom

Multiple R-squared: 1, Adjusted R-squared: 0.9946

F-statistic: 1.21e+02 on 2 and 456 DF, pvalue 254

The estimated effect of V2,V4, V5, V6 on the convert is 1.11999 3.25582 , -0.44712, 0.3371.

This means that for every 1% increase in V2 on X, there is a correlated 1.11% decrease in the incidence of Y. Similar to

V4, V5, V6

The standard errors for these regression coefficients are very small, and the t-statistics are very large (66.79, 271.46, 1.02

and 200, respectively). The p-values reflect these small errors and large t-statistics. And for both parameters, there is

almost zero probability that this effect is due to chance.

gives the variance in 0.001)

%update B

B = B + ((Z-X)/W) \* S;

B(isinf(B)) = 0;

%update beta

beta = B + L \* T;

%observations for logistics

m = beta \* X;

for i = 1:size(X,1)

temp =

makedist('Logistic', mu, mean(m(:,i)), 'sigma', abs(std(m(:,i))));

Z(:,i) = pdf(temp, Z(:,i));

R(:,i) = Z(:,i) - m(:,i);

end

%sampling lambda

Y = normpdf(Z, 0, 1);

Y = Y.^2;

Y = 1 + (Y - sqrt(Y \* (4 \* R + Y))) / (2 \* R);

lambda = Z;

for i = 1:6

Ztemp = R(:,i) \* Y(:,i);

Ztemp2 = R(:,i) ./ Y(:,i);

lambda(:,i) = Ztemp;

lambda(Z(:,i) > ones(size(Y(:,i))) / (1 + Y(:,i)))) =

if mean(lambda(:,i)) > 4/3

Z(:,i) = rightmost(Z(:,i), lambda(:,i));

else

Z(:,i) = leftmost(Z(:,i), lambda(:,i));

end

end

end

function Z = rightmost(U, lambda)

X = exp(-0.5 \* lambda);

Z = X;

% squeezing

for t = 1:length(X)-1

Z(t) = Z(t) - (t+1)^2 \* X(t)^(t+1)^2-1;

t = t+1;

Z(t) = Z(t) + (t+1)^2 \* X(t)^(t+1)^2-1;

end

Z(Z < U) = 0;

End

function Z = leftmost(U, Lambda)

H = 0.5 \* log(2) + 2.5 \* log(pi) - 2.5 \* log(Lambda) -

repmat(pi^2, 6, 1) / (2 \* Lambda) + 0.5 \* Lambda;

IU = log(U);

X = exp(-pi^2 / (2 \* Lambda));

Z = X;

K = Lambda / pi^2;

% squeezing

for t = 1:length(X)-1

Z(t) = Z(t) - K(t)^(t^2-1);

t = t+1;

Z(t) = Z(t) + K(t)^(t^2-1);

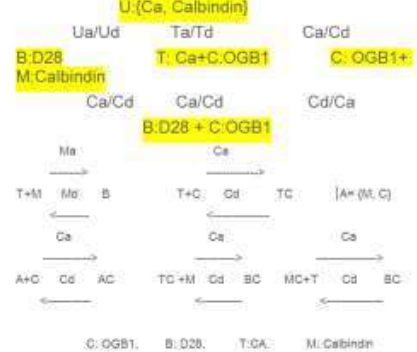
end

Z((reshape(H, 6, 1) + reshape(log(Z), 6, 1)) < reshape

pe(IU, 6, 1)) = 0;

End

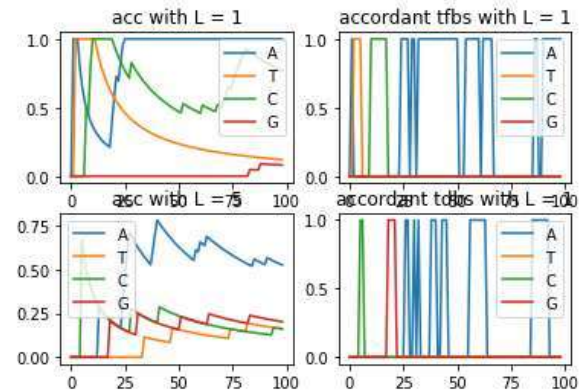
Mainly, I simplify one calciummodulin Activation by Calcium Transients of postsynaptic dendritic spines which finally constructed by 12 equations, first four as the clob, nlob binding to medium concentrated Ca and the second module as the similar clob and nlob but binding to high concentrated Ca binding sites followed by the fast binding of kinase II and the indicator OGB1. As it is the simplified version, its only based on the four independent binding site.



2. Cell reprogramming is usually a time lapse studied through gene expression data and DNA sequence data.

Through computing the reprogramming rate, it is shown that more reprogramming happen under the condition of inhibition of DNA methylation or the knowckdown of somatic transcription factors. In the first model, one fixed-variable-order Bayesian tree is constructed for the identification of transcription factor binding sites(TFBSs), while in the second model, the focus is on the expression data of the cell and transcription factors. This is mainly based on the process that

the promoters of ESCs can not only bounded by their own products but also activate other pluripotent genes and inhibit lineage specific genes. Thus, a markov model is applied to induce the reconstruction of transcription regulation in embryonic stem cell states, by the ectopic expression of factors and reprogram the differentiated cells.

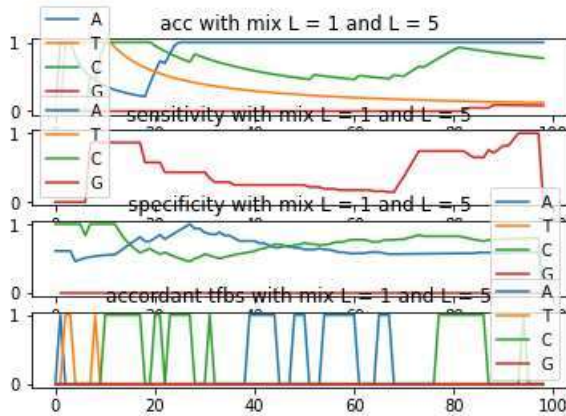


To realize the detection of binding site of DNA transcription factor, with homogeneous order 1 and 5 VOM(0.65,10), I first get the binding sites with the highest accuracy prediction peaks.  $X = \{A, T, C, G\}$ , and thus the  $d = 4$ . And using the mix model with pruning on KL scaled by threshold  $c$  on log scaled odds, the bayesian tree is for specifically to predict those at binding site(pruned level less than 3).

## D.Previous Work

1.Markoc chain of CaMKII circuit with regards to cognitive systems diseases especially about the MC and GC networks around hippocampus and dendrate gyrus. Please see one of my current work report following:

<https://www.overleaf.com/read/znwdjxppyzs>

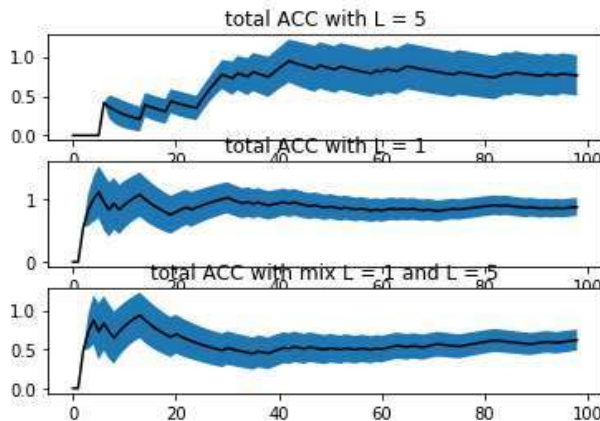


For the foreground dataset,  $L = 1$ , and each DNA sequence from  $X$  is predicted directly through the one before it while using the most easiest criteria, choosing the one with largest probability. For the background dataset,  $L = 5$ , and each DNA sequence from  $X$  is predicted through the previous five sequences before it while using the frequency of the respective subsequences combining Bayes Theory. And again, the highest peak frequency is chosen to be the bidding site with its probability approximated:

$$\hat{P}(X_j = x_j | X_{j-L}^{j-1} = x_{j-L}^{j-1}, \Omega_k) = \frac{n_k(x_{j-L}^{j-1})}{n_k(x_{j-L}^{j-1})},$$

$$P(x^N) = \prod_{j=1}^N P(X_j = x_j | X_{j-L}^{j-1} = x_{j-L}^{j-1}),$$

As the results, generally, the KL converges faster with  $L = 1$  and the mix model of order 1 and 5. In addition, the model is accumulated instead of step-wise, leading to the convergence not rising with the iteration. It is obvious that, on some specific TFBSs, the prediction is ven higher than others.



Algorithm: Stepwise Markov Ising model with lineage tree

1. The first step is to configure the epigenetic states of enquences through their expression, whehter "close" of "open" on any temporary cell state. (In our data, there are 64 cell states in all.)
2. The second step is to check the final state of each lineage tree, as the expression of modules maybe conflicted with each other, influenced by other cell's transcriptional regulatory network which might lead to cell death(we denoted as 0) while  $\epsilon$  denoted as the last state to the last states, which making 0 and  $n(66th)$  as the absorbing states.
3. The transition matrix is built according to reference [2]:

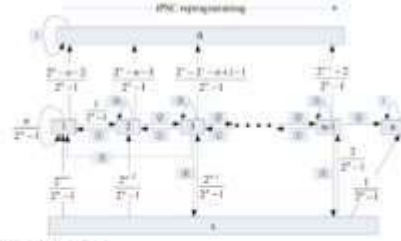


Figure 2 Reprogramming Markov Chain

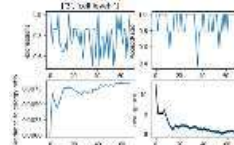
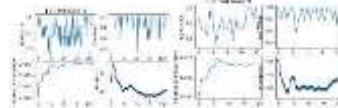
$$P(S_1 \rightarrow S_2) = \frac{1}{2} \left( \frac{1}{2} + \frac{1}{2} \right) = \frac{1}{2}$$

$$P(S_2 \rightarrow S_1) = \frac{1}{2} \left( \frac{1}{2} + \frac{1}{2} \right) = \frac{1}{2}$$

$$P(S_1 \rightarrow S_3) = \frac{1}{2} \left( \frac{1}{2} + \frac{1}{2} \right) = \frac{1}{2}$$

$$P(S_3 \rightarrow S_1) = \frac{1}{2} \left( \frac{1}{2} + \frac{1}{2} \right) = \frac{1}{2}$$

Note that in the first step, The transition states predicted through the highest probability. And in the second step, either probability(0 or  $\epsilon$  and further  $n$ ) over 0.5 will lead to the end of the markov process. Basically, it is based on the Ising model, choosing direction among  $\{P_1, P_2, P_3, P_5\}$  instead of the original random spin mchoise from  $\{-1, 1\}$  and the final fate of the cell is predicted through either  $\{0\}$  or  $\{n$  after  $\epsilon$ , i.e.  $P_4\}$ .



Among the 200 simulations, first level cell expression takes fewest amounts while the highest convergence. (Although the variance to energy ratio are quite similar for the three levels.). Generally, the Accept ratio is higher after the expression level goes to the lowest which is either when inhibition of DNA methylation exists or the knowckdown of somatic transcription factors occurs.

- [1]Novel Markov model of induced pluripotency predicts gene xpression changes in reprogramming Zhirui Hu,Minping Qian, Michael Q Zhang\*
- [2]A. Gohr, J. Grau, S. Arviv1, A. Shmilovici, S. Posch, and I.